Computational Study on the Influence of Non-Newtonian Nano fluids in Fluid Flow and Heat Transfer over a Permeable Surface with Injection and Suction

Imran Abbas[1]*, Shahid Hasnain[2], Muhammad Saqib[3], and Daoud Suleiman Mashat[4]

[1] Department of Mathematics, Air University, Islamabad, 44000 E-9, Pakistan

[2] Department of Mathematics, University of Chakwal, Chakwal, 48800, Pakistan

[3] Department of Mathematics, Khwaja Fareed University of Engineering & Information Technology, Rahim Yar Khan, 64200, Punjab, Pakistan

[4] Department of Mathematics, King Abdul-Aziz University, Jeddah, 21589, Saudi Arabia.

Abstract: This study examines the behaviour of Non-Newtonian Nano fluids in fluid flow and heat transfer over a permeable surface with injection and suction. The governing equations are converted into ordinary differential equations using a similarity approach and solved numerically with the Runge–Kutta–Fehlberg method. Copper (Cu), copper oxide (CuO),titanium oxide (TiO_2), and Aluminum oxide (Al_2O_3) nanoparticles are used in sodium carboxymethyl cellulose (CMC)/water as the base fluid to investigate the effects of power-law index, nanoparticle volume fraction, type, and permeability factor. The results indicate that Non-Newtonian nanofluids exhibit different behaviour than Newtonian nanofluids in the presence of suction and injection. Non-Newtonian nanofluid performs better than Newtonian

*Corresponding author: imranabbasattari@gmail.com

nanofluid in terms of heat transfer for injection and an impermeable plate, but changing the type of nanoparticles has a larger effect on heat transmission during suction. Furthermore, the deployment of Non-Newtonian Nano fluids in injection processes leads to a decrease in heat transmission for all three scenarios. Additionally, the study indicates that higher injection rates result in improved heat transfer, while increased suction rates lead to reduced heat transmission.

Keywords: Heat transfer, MHD, non-Newtonian, injection and suction.

Nomenclature

c constant

B_0 applied magnetic field

C_p specific heat

C_f skin friction coefficient

k^* thermal conductivity

Nu_x Nusselt number

$Pr = \frac{\nu}{\alpha}$ Prandtl number

T boundary layer temperature

T_w surface temperature

T_∞ ambient temperature

n power law index

u, v velocity components

f_w The constant value of transpiration

Subscripts

f fluids

nf nanofluids

Greek letters

ν kinematic viscosity

ρ fluid density

μ dynamic viscosity

σ electric charge density

ϕ dimensionless concentration

θ dimensionless temperature

$(\rho C_p)_f$ heat capacity of the fluid

$(\rho C_p)_p$ heat capacity of the nanoparticals

η dimensionless boundary layer thickness

β Casson parameter

1 Introduction

Non-Newtonian nanofluids refer to fluid suspensions containing solid nanoparticles that exhibit non-Newtonian behaviour. The distinct characteristics of nanofluids, like improved thermal conductivity and viscosity, have made them a popular choice for various engineering applications. Nanofluids with such unique properties, including enhanced thermal conductivity and viscosity, have become more prevalent in engineering applications for their practical utility. With their distinctive attributes, like increased thermal conductivity and viscosity, nanofluids of such kind have become increasingly favoured for a broad range of engineering applications. Enhanced thermal conductivity and viscosity are among the properties that make these types of nanofluids ideal for various engineering applications, resulting in their growing popularity [1, 2].

The use of nanofluids dates back to the early 1990s when Choi and Eastman first introduced the concept of nanofluids. The incorporation of nanoparticles in typical fluids, even in small amounts, can lead to significant improvements in their thermal performance. Since then, research into nanofluids has continued to expand, leading to the development of non-Newtonian nanofluids. Non-Newtonian fluids are those that do not follow the basic linear relationship between shear stress and shear rate, as specified by Newton's law of viscosity. Instead, the viscosity of non-Newtonian fluids changes with the rate of deformation, leading to a variety of complex flow behaviours. The addition of nanoparticles to these fluids can further enhance their non-Newtonian properties [3, 4].

In energy storage, non-Newtonian nanofluids have been used in the development of advanced battery and fuel cell technologies. The high thermal conductivity and viscosity of these fluids can improve the efficiency and stability of these devices, leading to longer lifetimes and reduced costs. In biomedical engineering, non-Newtonian nanofluids have been used in drug delivery systems and tissue engineering. The unique flow properties of these fluids can help to optimize drug delivery and improve the transport of nutrients and oxygen to living tissues. Nanofluid is a type of fluid that contains suspended nanoparticles, typically with sizes ranging from 1 to 100 nanometers, dispersed in a base fluid such as water, oil or glycol. These nanoparticles can be made of different materials, including metals, oxides, and carbon nanotubes, and they can enhance the thermal and electrical properties of the base fluid [5].

Non-Newtonian fluids known as "power law fluids" display a non-linear correlation among shear stress and shear rate. The flow behaviour of power law fluids in porous media can be described using the power law index, which finds the non-linearity of the fluid's rheology. The flow behaviour of power law fluids in porous media is important in various applications such as oil and

gas production, groundwater management, and environmental re-mediation. When determining in these areas, mathematical models and simulations can be utilized to forecast how power law fluids would behave in porous media under various circumstances. Sui *et al.* [6] carried out an experimental investigation to look into the distribution of heat in a non-Newtonian fluid with power-law behaviour's boundary layer. A mixed convection apparatus, which was created to enable the measurement of temperature distribution and flow velocity in the fluid's boundary layer, was used in the investigation. The study non-Newtonian fluid was a dilute aqueous solution of the power-law-behaving carboxymethyl cellulose (CMC). The researchers used an inclined plate and a moving conveyor as part of their experimental set-up to study the effects of shear flow, power-law viscosity, and temperature fluctuation. Meanwhile, Jalil *et al.* [7] investigations were undertaken with the goal of determining the properties and flow behaviour of a fluid that is shear-thinning over a boundary layer stretching surface that is smooth and permeable. They also look at how the fluid's permeability, surface stretching rate, and viscosity affect how the shear-thinning fluid flows. Ahmed *et al.* [8] used the shooting method and homotopic analysis, which were two separate mathematical techniques, to analyses the heat transfer and fluid flow of a power-law fluid over a radially stretched sheet. Guha *et al.* [9] investigated how different parameters, including the power-law index, the Grashof number, and the Prandtl number, affected the properties of flow and heat transmission. Meghdad *et al.* [10] examined the effect of heat radiation, or the movement of heat energy via electromagnetic waves like infrared radiation. When examining the behaviour of fluids, particularly at high temperatures or when working with materials that absorb or emit radiation, heat radiation is a crucial aspect to take into account.

Numerous researchers investigated the movement of a power-law fluid over a flat, porous plate while considering heat flux, suction, and injection. Heat flux refers to the transfer of thermal energy through a surface, while suction and injection refer to the removal or addition of fluid to the system. The researchers considered these factors in their study to better understand the behaviour of the fluid over the porous plate. They aimed to improve their understanding of fluid flow over porous surfaces, which has applications in fields such as chemical engineering, geology, and environmental science. The heat transfer characteristics of a power-law fluid flowing over a perpendicular plate are investigated with the impacts of radiation, a Darcy porous media, and chemical reaction. The research advances the topic of mixed convection heat transfer and offers helpful knowledge for planning and enhancing heat transfer procedures employing power-law fluids. O. G. Casson first proposed the Casson fluid, a non-Newtonian fluid model, in 1959. It is a specific kind of viscoelastic fluid with a yield stress, which means that up until a certain stress is applied,

it behaves as a solid before starting to flow like a liquid. Casson fluid is used in many different branches of research and engineering. These are a few instances: Casson fluid is used in the food business to simulate the behaviour of foods including sauces, ketchup, and mayonnaise. Casson fluid is used in the oil and gas sector to simulate the flow behaviour of drilling fluids and muds. The rheological characteristics of these fluids, which are utilized to lubricate and cool the drilling equipment, are crucial to the effectiveness of drilling operations. In biomedical engineering, Casson fluid is used to model the conduct of blood flow in arteries and veins. Overall, Casson fluid is a useful tool for understanding and predicting the behavior of complex fluids in various scientific and engineering applications [11–13]. The Casson fluid model, which takes into consideration the fluid's viscosity and yield stress, is frequently used to explain how blood behaves. According to the Casson model, the fluid has a yield stress that is non-zero below which no flow occurs, and beyond that stress, Shear stress and shear rate have a non-linear relationship.

Non-Newtonian models such as the Herschel-Bulkley model and the power law model have also been used to describe blood flow dynamics. The research may also explore the implications of this behaviour for various medical conditions or treatments, such as blood clotting disorders or blood rheology in micro-circulation [14, 15]. Several scientists have studied the Casson fluid's flow physiologies for a variety of applications, such as the steady and oscillatory flow of blood and the flow between rotating cylinders [16–18]. Abbas *et al.* [19] study investigated the impact of ethylene glycol and water base fluids on stagnation-point flow across a stretching sheet on the display of thermal radiation energy. The slip boundary condition is also considered in the study's inspection. Some researchers examined the magneto hydrodynamic (MHD) flow behavior within nanoparticles in porous channels while taking radiation's effect into consideration. The study focused on examining heat transfer events as well as the system's responses to injection, suction, and a transverse magnetic field [20] whereas, Guedri *et al.* [21] demonstrates the significant impact of various parameters on the flow, temperature, and concentration distributions in a micro polar fluid, which is crucial for understanding and optimizing heat and mass transfer processes in industrial applications. The study investigates the impact of nanoparticles, Prandtl number, and a magnetic field on the velocity and temperature profiles of a non-Newtonian Nano fluid using Tiwari and Das model, see [22]. The results demonstrate the influence of these factors on the Nussle number and skin friction parameters, presented through MATLAB simulations and graphical representations. Awan *et al.* [23] comparative study on the effect of rotational Prandtl host fluid flux involving aggregated Nano-particles and non-aggregated Nano-particles on a linear stretching surface. The convective movements of a fluid with linear viscosity in close proximity to a vertical isothermal plate. The

heat transfer phenomena are described using a generalized fractional constitutive equation, which incorporates a damped thermal and mass flux. An incompressible fluid impinging obliquely on an oscillatory stretching surface, studied by numerous scientists [24–26]. Abbas *et al.* [27] investigated the heat transmission and fluid flow properties of Newtonian and non-Newtonian Nano fluids across a permeable surface. The thermal and fluids characteristics of Nano-fluids, which contain nanoscale particles suspended in them, are distinct from those of pure fluids. The goal of the study is to comprehend how these particles effect heat transfer and fluid flow via a permeable surface when a magnetic field is present. MHD is a term used to explain the behavior of liquid metals and plasmas, two examples of fluids that conduct electricity. MHD effects, including the Hall Effect, magnetic drag, and Lorentz force, can occur when a fluid moves through a magnetic field. The heat transfer characteristics of a Maxwell micro polar fluid with hybrid nanomaterials are investigated as it flows over an exponentially stretching surface, by [28–30].

Heat transfer is a significant concern in modern technology, arising from temperature variations between different physical processes, see Akbar *et al.* [31]. Whereas, the design of reactors and mixers in chemical engineering can be optimized using stagnation point flow [32–37]. A numerical analysis on the flow of Sutterby fluid in two dimensions that was constrained to a stagnation point and exposed to an angled magnetic field and heat radiation was conducted by Sabir *et al.* [38]. A computer analysis of the flow of a fictitious plastic nano-liquid towards a flexible Riga sheet at a stagnation point was done by Azad *et al.* [39]. The enhancement of heat transfer in channel flow by replacing the smooth duct with a corrugated duct. The study demonstrates that using periodic corrugations in rectangular ducts significantly improves thermal-hydraulic behaviours, leading to enhanced flow mixing and heat transfer efficiency. The study focuses on a numerical investigation of the impact of water-based Al_2O_3 Nano fluids on flow characteristics and heat transfer enhancement in rectangular corrugated channels. [40–42] Ozbolat *et al.* [43] utilizes numerical methods to investigate the flow field and heat transfer characteristics of water within two-dimensional sinusoidal and rectangular corrugated wall channels. Bilen *et al.* [44] examines the effects of swirl generators, positioned at the pipe inlet and featuring various swirl angles (0°, 22.5°,41° & 50°), on heat transfer and fluid flow characteristics in pipe flow.

In this work, we used the Tiwari and Das model which introduces innovative elements by incorporating the cession fluid and stagnation flow into the study. The synergy of the cession fluid with the magnetic field and Nano fluid flow adds a new dimension to the study, while the stagnation flow introduces additional complexity, elevating the significance and practicality of the study's findings. The results and analyses obtained in this research are meticulously presented

using MATLAB, a widely-recognized software tool for numerical simulations and data analysis. The study significantly enhances our comprehension of the behaviour of non-Newtonian Nano fluids under the influence of a magnetic field, and provides valuable insights into how various parameters impact velocity and temperature distributions. Additionally, the research sheds light on the heat transfer and friction characteristics of the fluid flow, crucial aspects in a wide range of industrial and engineering applications.

2 Formulation of problem

In this problem, a stationary flat plate is considered, which is permeable to fluid flow. The fluid motion near the surface is two-dimensional and steady, and the fluid is a mixture of water and CMC particles, referred to as a Nano fluid. The flow is laminar, meaning that the fluid particles move in an orderly, non-turbulent manner. The fluid is also incompressible, meaning that its density remains constant regardless of changes in pressure. The model used to describe the flow accounts for slippage between the fluid phase and the nanoparticles, meaning that the movement of nanoparticles is not restricted to that of the fluid. Figure.1 illustrates the graphical model and coordinate arrangement, where stream velocity and ambient temperature are denoted by their respective representations.

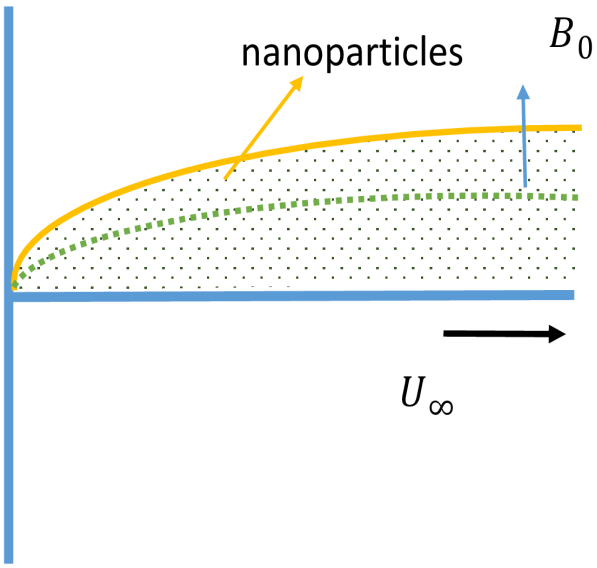

Fig. 1: Geometrical setup of the problem.

Being within the above constraints, governing equations of the above modelled problem are as

follow:

$$u^*\frac{\partial T^*}{\partial x}+v^*\frac{\partial T^*}{\partial y}=\alpha_{nf}\frac{\partial}{\partial y}\left(|\frac{\partial T^*}{\partial y}|^{n-1}\frac{\partial T^*}{\partial y}\right). \tag{1}$$

$$\frac{\partial u^*}{\partial x}+\frac{\partial v^*}{\partial y}=0, \tag{2}$$

$$u^*\frac{\partial u^*}{\partial x}+v^*\frac{\partial u^*}{\partial y}=\left(1+\frac{1}{\beta}\right)\frac{\mu_{nf}}{\rho_{nf}}\frac{\partial}{\partial y}\left(|\frac{\partial u^*}{\partial y}|^{n-1}\frac{\partial u^*}{\partial y}\right)-\frac{\sigma_{nf}B_0^2}{\rho_{nf}}(u^*-U_\infty)+U^*\frac{\partial U^*}{\partial x}, \tag{3}$$

Boundary conditions :

$$u^*\to U_\infty \quad as \quad y\to\infty,\ u^*=0, \quad v^*=V_W(x) \quad as \quad y=0. \tag{4}$$

$$-k_{nf}\frac{\partial T^*}{\partial y}=h_f(T_f-T_w) \quad at \quad y=0,\ T^*\to T_\infty \quad as \quad y\to\infty. \tag{5}$$

3 Thermo Physical Characteristic

Thermo-physical characteristics refer to the physical and thermal properties of a substance, which can be measured and quantified. These properties can include thermal conductivity, specific heat capacity, viscosity, density, boiling point, melting point, and more. These characteristics describe how a substance behaves when exposed to temperature changes or other thermal and physical condition. Utilized in the discussion at hand and are described as [40].

$$\alpha_{nf}=\frac{k_{nf}}{(\rho C_p)_{nf}},\mu_{nf}=\frac{u}{(1-\varphi)^{2.5}},\frac{k_{nf}}{k_f}=\frac{(k_s+2k_f)-2\varphi(k_f-k_s)}{(k_s+2k_f)+\varphi(k_f+k_s)}, \tag{6}$$

$$(\rho C_p)_{nf}=(1-\varphi)(\rho C_p)_f+\varphi(\rho C_p),\rho_{nf}=(1-\varphi)\rho_f+\varphi\rho_s. \tag{7}$$

4 Solution Approach

The following transformation laws are used to convert governing equations into Dimensionless form.

$$\psi=(U_\infty^{2n-1}vf_x)^{\frac{1}{n+1}}f(\eta),\ u^*=\frac{\partial\psi}{\partial y}, \quad v^*=-\frac{\partial\psi}{\partial x}, \tag{8}$$

$$\eta=\left(\frac{U_\infty^{2-n}}{v_f x}\right)^{\frac{1}{n+1}}y, \quad \theta=\frac{T^*-T_\infty}{T_f-T_\infty} \tag{9}$$

Solving equations (1-5) with the help of similarity transformation also solving with boundary conditions obtained following results are:

$$\frac{1}{A_4 A_1}(|f''|^{n-1}f'')' + \frac{1}{n+1}f''f - M^2\frac{\sigma_{nf}}{\sigma_f}(f'-1) = 0 \tag{10}$$

$$-\frac{A_3}{Pr_f A_2}(|f''|^{n-1}\theta')' + \frac{1}{n+1}f\theta' = 0 \tag{11}$$

where

$$\begin{gathered}\frac{\sigma_{nf}}{\sigma_f} = 1 + \frac{3\varphi\left(\frac{\sigma_s}{\sigma_f}\right) - 1}{\left(\frac{\sigma_s}{\sigma_f}+2\right) - \varphi\left(\frac{\sigma_s}{\sigma_f}\right) - 1}, \\ M = \sqrt{(\frac{xB_0^2}{\rho_{nf}})} \quad and \quad \lambda = \frac{Q_0}{\rho C_p}\end{gathered} \tag{12}$$

$$A_1 = \frac{1}{(1-\varphi) + \frac{\varphi\rho_s}{\rho_f}}, \quad A_2 = -\frac{1}{(1-\varphi) + \varphi\frac{(\rho C_p)_s}{(\rho C_p)_f}}, \tag{13}$$

$$A_3 = -\frac{(\frac{k_s}{k_f}+2) - 2\varphi(1-\frac{k_s}{k_f})}{(\frac{k_s}{k_f}+2) + \varphi(1-\frac{k_s}{k_f})}, \quad A_4 = \frac{1}{(1-\varphi)^{2.5}}. \tag{14}$$

Boundary conditions:

$$f(0) = f_w, \quad f'(0) = 0, \quad f'(\infty) = 1, \tag{15}$$

$$\theta'(0) = A_3 a(1-\theta(0)), \quad \theta(\infty) = 0. \tag{16}$$

where $f_w = 0, 1, -1$ stands for impermeable sheet suction and injection respectively.

5 Engineering Quantities of Interest

In this section, we will investigate the physical properties and behaviours of the local Nusselt number and skin friction coefficient. This analysis will involve examining how these parameters vary in response to different flow conditions and geometries. By studying their behaviour, we can gain insights into the underlying physical mechanisms that drive heat transfer and fluid flow in a given system. This exploration can be especially helpful when analytical solutions are not available or when the system's complexity precludes an analytical approach. We will examine how these two parameters are related to the transfer of heat and momentum in fluid mechanics, and how they vary with changes in the flow conditions and geometries of the system being studied. By gaining a

deeper understanding of the physical principles governing these coefficients, we can better predict and optimize the heat transfer and flow dynamics in a wide range of engineering applications. In this section, we will explore the physical characteristics and behaviour of the local Nussle number and skin friction coefficient. We will examine how these two parameters are related to the transfer of heat and momentum in fluid mechanics, and how they vary with changes in the flow conditions and geometries of the system being studied. By gaining a deeper understanding of the physical principles governing these coefficients, we can better predict and optimize the heat transfer and flow dynamics in a wide range of engineering applications. The following quantities are defined as:

$$C_{fx} = -\frac{2\tau_w}{\rho_f U^2}, \qquad Nu_x = \frac{x q_w}{k_f(T_w - T_\infty)}, \tag{17}$$

where

$$\tau_w = \mu_{nf}\left(|\frac{\partial u^*}{\partial y}|^{n-1}\frac{\partial u^*}{\partial y}\right)_{y=0}, \quad q_w = -k_{nf}\left(\frac{\partial T^*}{\partial y}\right)_{y=0}. \tag{18}$$

By employing similarity transformation, the obtained results are as follows:

$$\begin{aligned} Cf_x Re_x^{\frac{1}{n+1}} &= -2\frac{\mu_{nf}}{\mu_f} f''(0)|f''(0)|^{n-1}, \\ Nu_x Re_x^{\frac{-1}{n+1}} &= -\frac{k_{nf}}{k_f}\theta'(0). \end{aligned} \tag{19}$$

6 Validation and Discussion

The data Table 1,shows the comparison results between results.Ejaz *et al.* [22] and present results. This table show our results is better than previous results. Figure 2 demonstrate that the current results are more precise and reliable compared to the previous findings.

Table2 are appears to be presenting numerical results $f''(0)$, for various combinations of factors. Let's break down what these quantities and parameters mean: $f''(0)$ represents the second derivative of the velocity profile at the wall. This quantity is important in fluid mechanics because it determines the rate of momentum transfer between the fluid and the wall. Negative values of$f''(0)$ indicate that the fluid is being decelerated at the wall (i.e., the fluid velocity is decreasing as it approaches the wall).

f_w	Chen *et al.* [20]	Ejaz *et al.* [22]	Present results
0	-0.4438	-0.4437	-0.4436
0.1	-0.4737	-0.4436	-0.4435
0.5	-0.6031	-0.6021	-0.6010
1	-0.7864	-0.7862	-0.7861

Table 1: Explore the variation $f''(\eta)$ at n = 0.85, for different values of the f_w.

7 Results

7.1 Variational impact on Skin and local Nusselt numbers

The ratio of convective to conductive heat transfer across a boundary is represented by the Nusselt number, a dimensionless quantity in heat transfer. It is employed to describe the improvement in heat transmission caused by the presence of nanoparticles in a fluid. Figures 3, 4, 5 depict the relationship between the Nusselt number and the volume percentage of nanoparticles for various nanoparticle types in three distinct cases: impermeable surface, suction, and injection.

The percentage of the fluid's volume that is made up of nanoparticles is known as the volume fraction. A volume fraction of 0.01, for instance, indicates that nanoparticles make up 1% of the fluid. When a surface is impermeable, it is thought that nanoparticles cannot cross the boundary layer and only have an impact on heat transfer at the fluid-solid interface. When nanoparticles are permitted to enter the boundary layer and interact with the flow in the suction and injection situations, the convective heat transfer is altered. Suction describes a situation in which fluid is sucked into the surface, whereas injection describes a situation in which fluid is discharged from the surface. The plot shows how the Nusselt number changes as the volume fraction of nanoparticles is varied for each of these three cases. The slope of the curve represents the effectiveness of the nanoparticles in enhancing the heat transfer. A steeper slope indicates a more significant enhancement of heat transfer as the volume fraction of nanoparticles increases. Non-Newtonian fluid has an impact on suction and the Nusselt number augmentation on impermeable surfaces. On the different side, heat transmission during injection is significantly reduced by non-Newtonian Nano fluid. The type of Nano fluids or their volume fraction had no discernible effect on local Nusselt number augmentation during suction or injection. When titanium dioxide or aluminum

oxide nanoparticles are introduced to the suction fluid, heat transmission is reduced. Suction generally has better heat transfer characteristics than the other two examples (e.g., Nusselt number, temperature gradient).

In the case of suction, the Nusselt number typically decreases as the suction velocity increases. This is because suction removes some of the fluid that would otherwise be in contact with the heated surface, reducing the rate of heat transfer. However, if the suction is strong enough, it can also cause turbulence and increase the rate of heat transfer, leading to an increase in the Nusselt number. In the case of injection, the Nusselt number typically increases as the injection velocity increases. This is because the injected fluid mixes with the fluid in contact with the heated surface, increasing the rate of heat transfer. However, if the injection velocity is too high, it can cause the flow to become turbulent and reduce the efficiency of heat transfer, leading to a decrease in the Nusselt number.

Figures 6, 7, & 8 determine the effects of various nanoparticles on the local friction factors of two different classes of working fluids, Newtonian and non-Newtonian. Non-Newtonian Nano fluids have a higher local friction factor than Newtonian fluids. Moreover, the local friction factor values rise as the amount of nanoparticles in fluids used for transportation increases. The relationship between the volume fraction of different types of nanoparticles added to a fluid and the skin friction that results on a surface is demonstrated by the plot of skin friction against nanoparticle volume fraction. Understanding fluid dynamics and the effectiveness of fluid flow in various engineering applications requires an understanding of skin friction, which is the resistance that a fluid encounters when it flows over a surface. The different types of nanoparticles included in the plot likely have different physical and chemical properties that can affect the behaviour of the fluid when they are added to it. For example, nanoparticles with a higher density may cause more turbulence in the fluid, leading to higher skin friction.

The local friction factor for rising the volume fraction of nanoparticles is peak value for suction and deepest for injection. Furthermore, associated to other nanoparticles, the copper nanoparticle has a larger local friction factor. Alumina nanoparticles have a lower local friction factor than other nanoparticles. In the case of a fluid injection, the skin friction coefficient is typically higher than in the case of suction. This is because when a fluid is injected into a boundary layer, it typically disrupts the flow and creates turbulence, which leads to increased shear stresses and higher skin friction coefficients. Friction coefficients.

7.2 Impact of investigated parameters on flow velocity

In Figures 9, 10 & 11, the impact of nanoparticle volume fraction is shown for three different values impermeable surface, suction, and injection, denoted by $f_w = 0, 1, \& -1$, respectively. When the volume fraction of nanoparticles is increased, the fluid velocity increases for impermeable surfaces and suction. This could be due to the fact that the nanoparticles have a larger surface area than the fluid molecules themselves, leading to an increase in the effective viscosity of the fluid. This, in turn, causes the fluid to move faster over the impermeable surfaces or towards suction. On the other hand, when injection is considered, the opposite trend is observed. This could be due to the fact that the nanoparticles act as obstacles to the fluid flow, impeding its movement and causing a decrease in velocity. When impermeable plates (plates that do not allow fluids to pass through) are used in conjunction with Newtonian nanofluids (fluids containing nanoparticles that exhibit Newtonian behaviour), the velocity gradient over a flat plate is not affected, but the thickness of the boundary layer is reduced. The velocity gradient refers to the rate at which the velocity of the fluid changes as it moves across the flat plate. The boundary layer is the thin layer of fluid adjacent to the surface of the plate, where the velocity of the fluid is affected by the presence of the plate.

When impermeable plates are used, they prevent the fluid from penetrating the plate and thus do not affect the velocity gradient. On the other hand, when Newtonian Nano fluids are used, they reduce the viscosity of the fluid and result in a thinner boundary layer. This reduction in boundary layer thickness can be beneficial in many applications, such as reducing drag and increasing heat transfer efficiency. Figure 12 shows how permeability affects both Newtonian and non-Newtonian Nano fluids' velocity profiles. The velocity at the wall (f_w) is zero in the case of impermeable walls and suction, and the velocity profile close to the wall is parabolic. The slope of the velocity profile's second derivative, $f''(\eta)$, which is negative, indicates how quickly the slope is changing. The velocity at the middle of the channel increases and the velocity gradient near the wall gets more negative as the slope of the velocity profile steepens (i.e., the magnitude of $f(\eta)$ grows). As a result, the boundary layer, or the region of fluid near the wall where the velocity is noticeably lowered due to viscous effects, becomes thinner. This means that the fluid near the wall is more severely affected by the wall. The amount of fluid being evacuated from the channel is thus reduced.

When impermeable barriers are present and injection occurs, neither the velocity at the wall nor the velocity profile close to the wall are parabolic. Depending on the specifics of the flow, the second derivative of the velocity profile ($f''(\eta)$) might either be positive or negative. In general, the impact of $f''(\eta)$ on f_w is minimal if the injection rate is low. Yet as the injection rate goes up, $f"(\eta)$ gets bigger and the velocity profile curves out farther towards the wall. Both the velocity at

the wall and the thickness of the boundary layer may increase as a result of this. The fluid can permeate the wall and flow along it if the channel has permeable walls. This alters the velocity profile close to the wall and can confuse the way $f''(\eta)$ works. Yet, in general, the boundary layer's thickness and the steepness of the velocity profile close to the wall continue to influence how $f''(\eta)$ affects f_w.

Figure 13 demonstrates the non-dimensional velocity of two types of Nano fluids (Newtonian and non-Newtonian) at numerous values of the magnetic interaction parameter M. The results reveal that as the magnetic field strength increases, the fluid velocity also increases for both Nano fluid types. However, it is observed that the boundary layer thickness also increases with higher magnetic field strength, resulting in a reduction of the Nano fluid's velocity.

Figures 14, 15 & 16 depict the second derivative of a function $f(\eta)$ represents the rate of change of the slope of the function with respect to the independent variable η. A stagnation point occurs when the velocity of a fluid flow becomes zero. The effects of $f''(\eta)$ with a stagnation point for impermeable suction and injection can be analyzed using the following cases:

- **Case 1: Impermeable Suction and Injection with** $f''(\eta) > 0$ If $f''(\eta) > 0$, then the slope of the function $f(\eta)$ is increasing. This indicates that the fluid flow is accelerating as it moves away from the stagnation point. In the case of impermeable suction and injection, the fluid is being pumped into or out of the stagnation point. Therefore, the velocity of the fluid increases as it moves away from the stagnation point due to the continuous injection or suction of fluid. This leads to a flow with a positive acceleration.

- **Case 2: Impermeable Suction and Injection with** $f''(\eta) < 0$ If $f''(\eta) < 0$, then the slope of the function $f(\eta)$ is decreasing. This indicates that the fluid flow is decelerating as it moves away from the stagnation point. In the case of impermeable suction and injection, the fluid is being pumped into or out of the stagnation point. Therefore, the velocity of the fluid decreases as it moves away from the stagnation point due to the continuous injection or suction of fluid. This leads to a flow with a negative acceleration.

- **Case 3: Impermeable Suction and Injection with** $f''(\eta) = 0$ If $f''(\eta) = 0$, then the slope of the function $f(\eta)$ is constant. This indicates that the fluid flow maintains a constant velocity as it moves away from the stagnation point. In the case of impermeable suction and injection, the fluid is being pumped into or out of the stagnation point. Therefore, the velocity of the fluid remains constant as it moves away from the stagnation point due to the continuous injection or suction of fluid. This leads to a flow with zero acceleration.

Figures 17 & 18 show the Blasius flow of Newtonian and non-Newtonian Nano fluid at various values of the Casson parameter. It is known as the Casson parameter, which is the square root of the yield stress divided by the plastic viscosity, and it is a rheological parameter that describes the flow behaviour of non-Newtonian fluids.

The Casson parameter is often used to model the velocity profiles of fluids in various flow situations, including suction and injection. It is particularly useful for modelling the behaviour of fluids with complex flow properties, such as blood and other biological fluids, as well as some industrial fluids. In general, the Casson parameter affects the velocity profiles of fluids in suction and injection situations in the following ways: Increase in Casson parameter leads to an increase in the yield stress of the fluid. This causes the velocity of the fluid to decrease near the wall, resulting in a steeper velocity profile.

In suction situations, as the Casson parameter increases, the velocity of the fluid decreases near the wall. This results in a higher suction force, which can cause the fluid to be drawn closer to the wall. In injection situations, as the Casson parameter increases, the velocity of the fluid decreases near the wall. This results in a higher injection force, which can cause the fluid to be pushed away from the wall.

7.3 Effects on Temperature profile

Figures19 & 20 present temperature profiles for suction, injection, and impermeable surfaces in different fluid and nanoparticle configurations. For Newtonian fluid with suction and impermeable plates, the dimensionless temperature initially reductions and then increases. The same trend is detected for both Newtonian and non-Newtonian fluids on impermeable plates. However, when non-Newtonian fluid is used on impermeable plates with increased volume percentage of nanoparticles, the dimensionless surface temperature decreases. Regarding suction, the volume percentage of nanoparticles has minimal impact on the plate surface temperature.

However, when non-Newtonian fluid is utilized, it significantly reduces the temperature and results in a thinner boundary layer compared to Newtonian fluid. In Figures 21 & 22 the temperature profiles for impermeable, suction, and injection surfaces are presented for various power-law index values. The results show that impermeable surfaces enhances and suction benefit from an increase in non-dimensional temperature, while injection surfaces do not. In the case of suction, the velocity profile is thinner compared to the no-suction case. This is because suction removes fluid from the boundary layer, resulting in a decrease in the thickness of the boundary layer.

The velocity near the surface is also increased due to the removal of the slower-moving fluid in the boundary layer. This effect is more pronounced for power-law fluids with higher power law index values

beta	M	*epsilon*	fw	A	pr	n	bvp4c	Shooting
1	0.1	0.1	0.1	0.5	1.0	0.85	1.1828327	1.1355031
2							1.1828328	1.1828336
3							1.229482	1.229481
	0.2						1.077498	1.077499
	0.5						0.798767	0.798768
	1.0						0.044135	0.044139
		0.1					1.077498	1.077499
		0.3					1.000720	1.000719
		0.5					0.906847	0.906848
			0.3				1.221272	1.221271
			0.5				1.299390	1.299391
			1.2				1.543654	1.543652
				0.2			1.135504	1.135503
				0.4			1.135504	1.135503
				0.8			1.133991	1.133992
					0.9		1.135504	1.135503
					0.7		1.135504	1.135503
					0.3		1.135504	1.135503
						0.85	1.135504	1.135503
						0.83	1.133991	1.133992
						1	1.133990	1.133991

Table 2: Numerical results of $f''(\eta)$, and for different values of β, M, ϵ, Pr, n

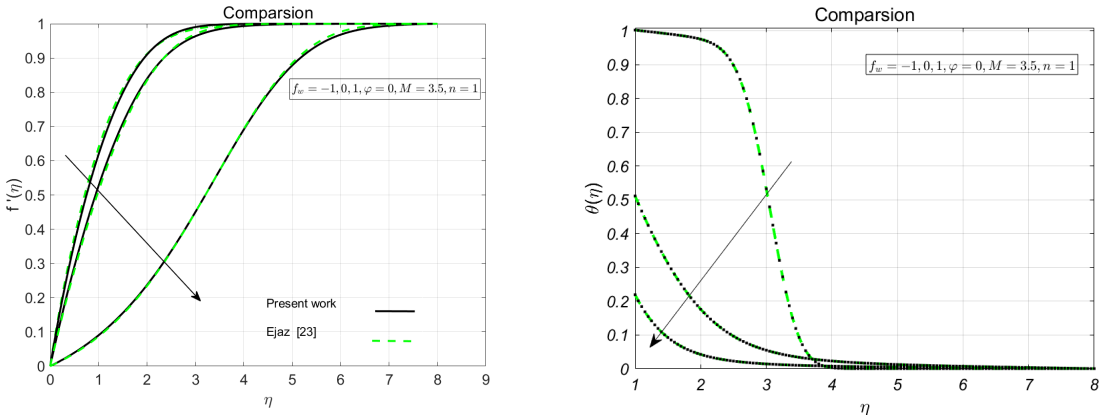

(a) A profile of velocities.

(b) A graph of temperatures.

Fig. 2: Variation in permeability have an impact on the velocity and temperature profiles.

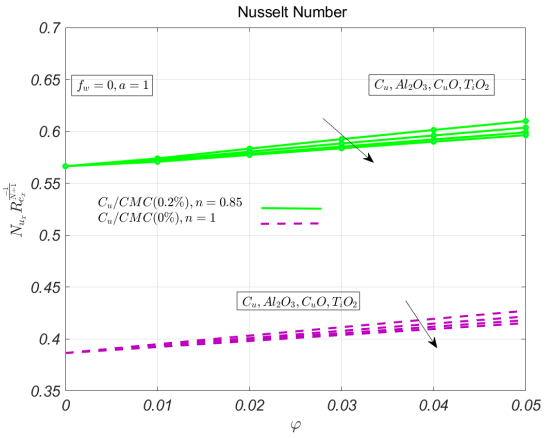

Fig. 3: several nanoparticles effects on the Nussle numbers for imperable

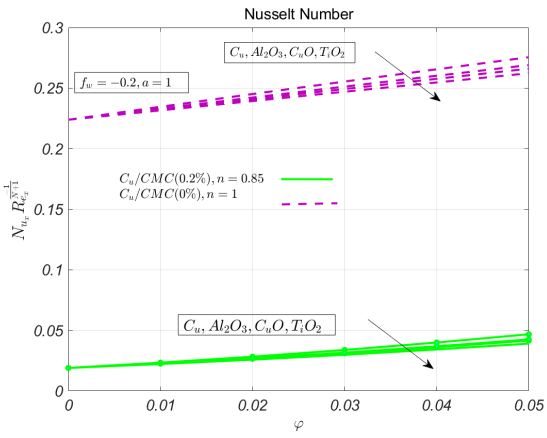

Fig. 4: several nanoparticles effects on the Nussle numbers for injection

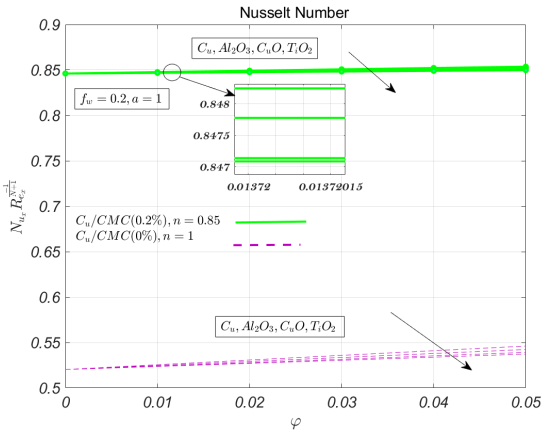

Fig. 5: several nanoparticles effects on the Nussle numbers for suction

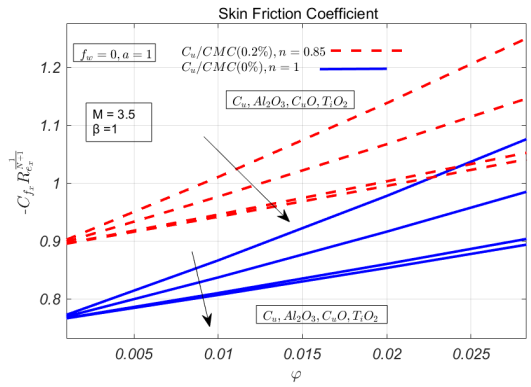

Fig. 6: Impact of different nanoparticles on skin friction number for imperable

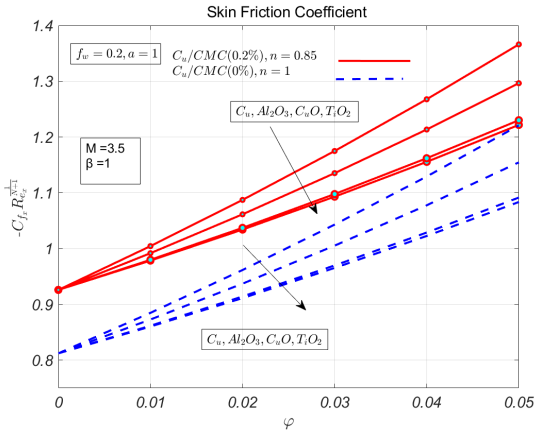

Fig. 7: Impact of different nanoparticles on skin friction number for suction

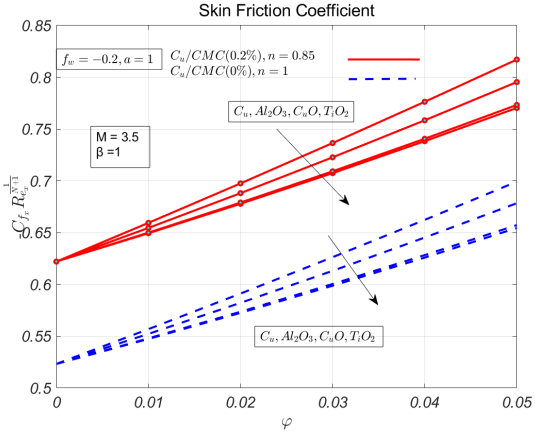

Fig. 8: Impact of different nanoparticles on skin friction number for injection

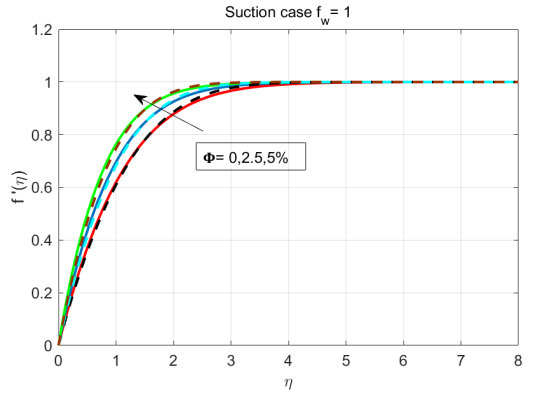

Fig. 9: Effect of $f''(\eta)$ with φ for suction

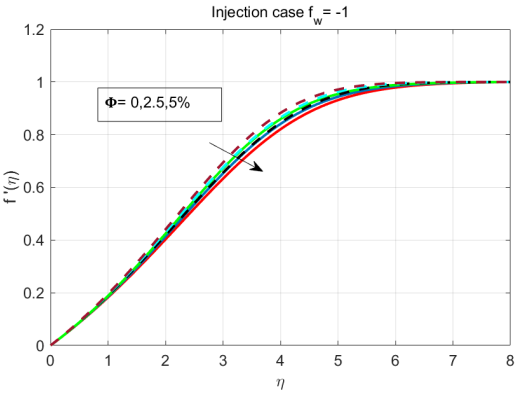

Fig. 10: Effect of $f''(\eta)$ with φ for injection

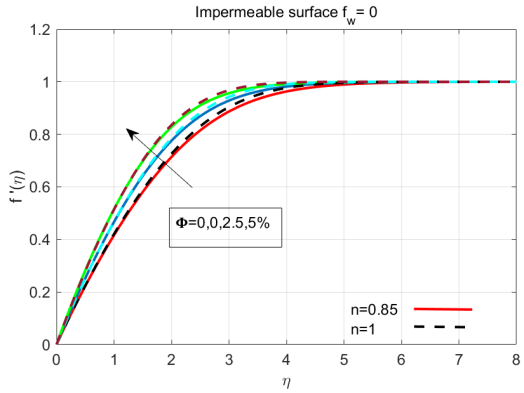

Fig. 11: Effect of $f''(\eta)$ with φ for imperable

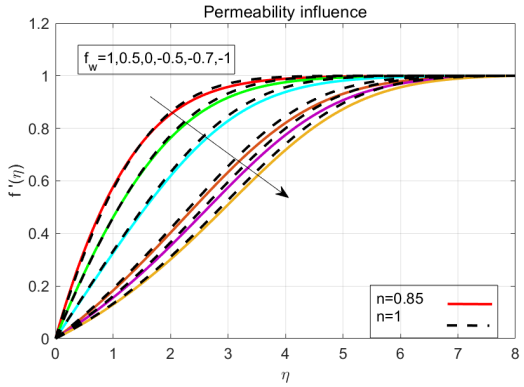

Fig. 12: Effect of $f''(\eta)$ with f_w for imperable suction and injection

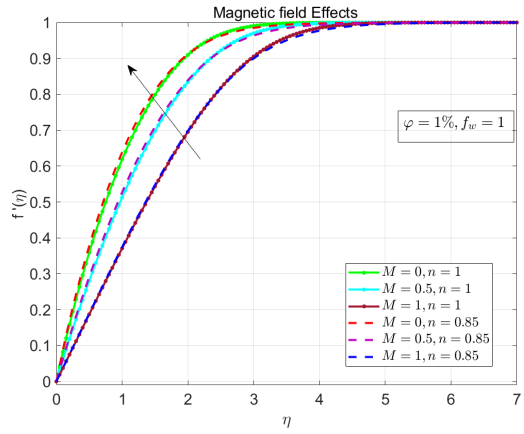

Fig. 13: Effects of $f''(\eta)$ with magnetic field M

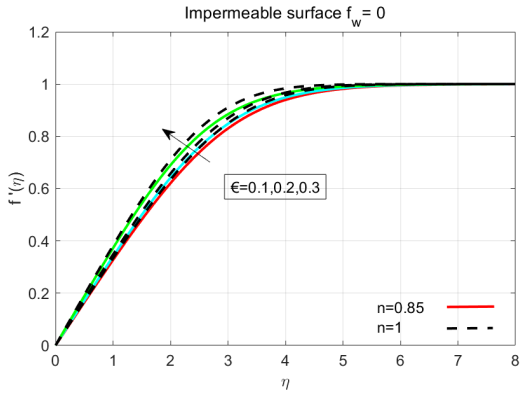

Fig. 14: Effects of $f''(\eta)$ with ϵ for imperable

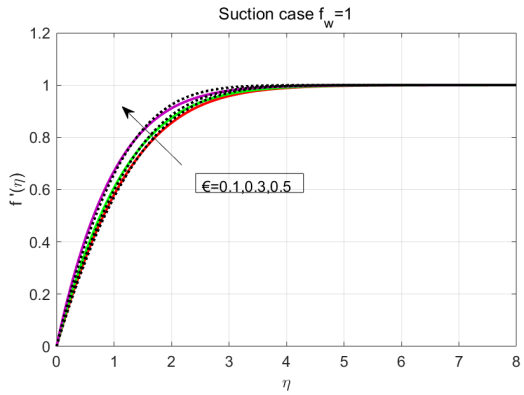

Fig. 15: Effects of $f''(\eta)$ with ϵ for suction

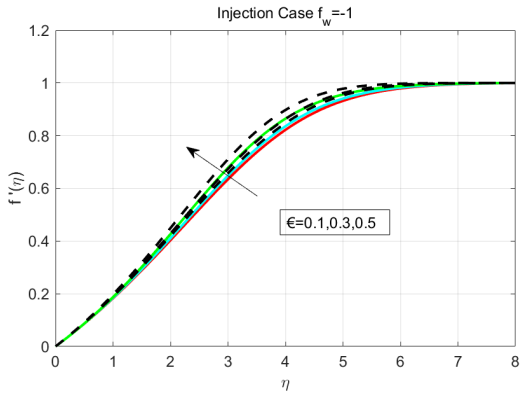

Fig. 16: Effects of $f''(\eta)$ with ϵ injection

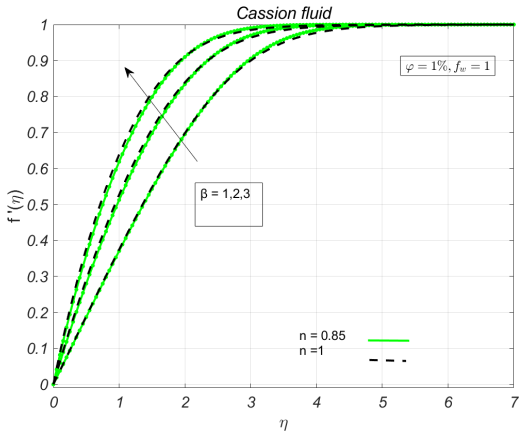

Fig. 17: Effects of $f''(\eta)$ with β for suction

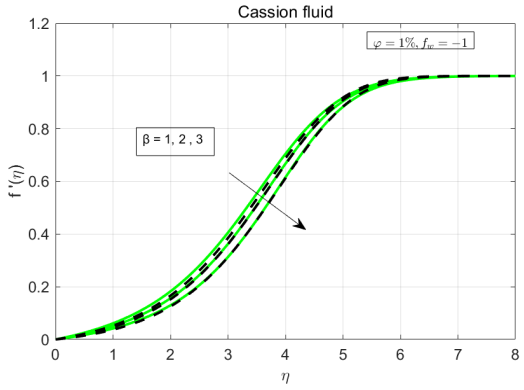

Fig. 18: Effects of $f''(\eta)$with β for injection

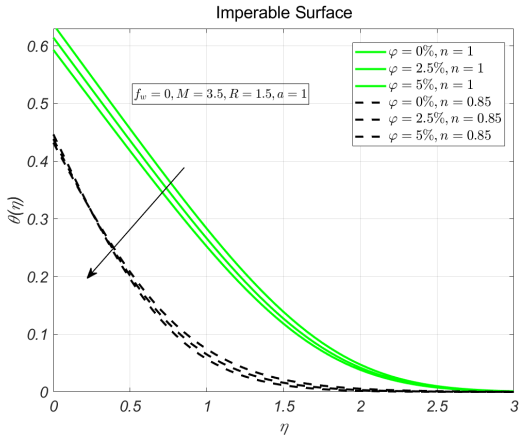

Fig. 19: Effects of $\theta''(\eta)$ with φ for imperable suction

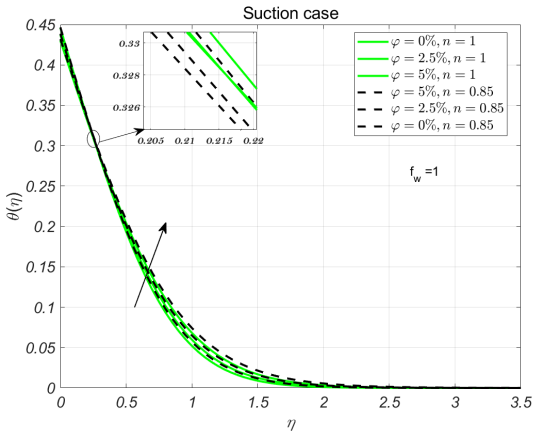

Fig. 20: Effects of $\theta''(\eta)$ with φ for suction

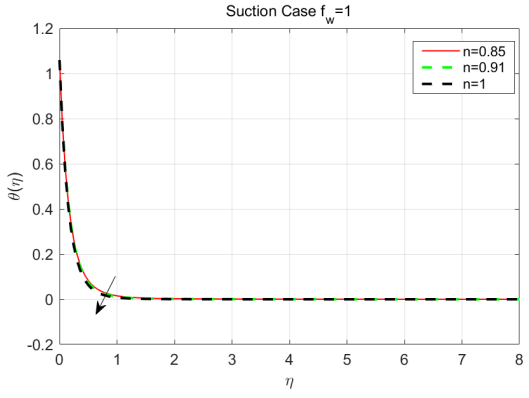

Fig. 21: Effects of with n for suction

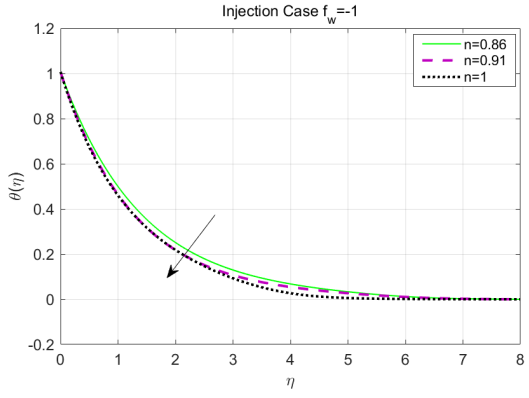

Fig. 22: Effects of $f''(\eta)$ with n for injection

8 Conclusion:

This work introduces ground breaking elements by combining the cassion fluid and stagnation flow into the study. The interaction of cassion fluid with the magnetic field and Nano fluid flow adds a novel aspect to the research, while the inclusion of stagnation flow brings in extra complexity, making the findings more significant and practical. The results and analyses obtained in this research are meticulously presented using MATLAB, a widely-recognized software tool for numerical simulations and data analysis. The study greatly enhances our understanding of the behavior of non-Newtonian Nano fluids under the influence of a magnetic field, and provides valuable insights into how different parameters affect velocity and temperature distributions. Moreover, the research sheds light on the heat transfer and friction characteristics of the fluid flow, which are crucial in a wide range of industrial and engineering applications. Based on the results of the study, it can be concluded that the behavior of non-Newtonian Nano fluids with pseudo-plastic properties is affected by the concentration of nanoparticles, as well as the shear rate and temperature. The viscosity of the Nano fluid decreases as the concentration of nanoparticles increases, and the rate of decrease is more pronounced at higher shear rates. Additionally, the viscosity decreases as the temperature increases. We found that the alumina and Titania Nano fluids exhibited shear-thinning behavior, meaning that their viscosity decreased as the shear rate increased. The copper and cupric oxide Nano fluids, on the other hand, exhibited shear-thickening behavior, meaning that their viscosity increased as the shear rate increased. Overall, the study provides important insights into the behavior of non-Newtonian Nano fluids with pseudo-plastic properties, which could have significant implications for a range of industrial and engineering applications, including heat transfer and fluid flow. The numerical methods used in the study, such as the similarity technique and the Runge-Kutta-Fehberg methods, could also be useful for analyzing the behavior of other complex fluids and materials. The following points:

- The effect of nanoparticles on fluid velocity depends on the case (suction, impermeable surface, or injection), and the suction parameter can reduce the boundary layer thickness.
- Despite having stronger heat conduction than CuO, Al_2O_3has inferior heat transfer properties.
- Heat transfer is not always enlarged when the volume fraction of np is increased. It was found that the suction case heat transfer was lowered when the volume percentage of Al_2O_3 and TiO_2 nanoparticles was increased.

- When non-Newtonian fluid is used in injection procedures, heat transfer is reduced and friction is increased.
- In the same circumstances, non-Newtonian nanofluids have a larger local friction factor value than Newtonian fluids

References

[1] Zainali, A., Tofighi, N., Shadloo, MS., et al. "Numerical investigation of Newtonian and non-Newtonian multiphase flows using ISPH method" *Computer Methods in Applied Mechanics and Engineering*, **254**(1), pp. 99–113, (2013).

[2] Choi, TJ., Kim, SH., and Jang SP. "Specific Heat Capacity and Density of Nanofluids" *In Fundamentals and Transport Properties of Nanofluids*, pp. 282–300, (2022).

[3] Dharmaiah, G., Dinarvand, S., Prasad, JR., et al. "Non-homogeneous two-component buongiorno model for nanofluid flow toward Howarth's wavy cylinder with activation energy" *Results in Engineering*, **17**(1), pp. 100879, (2023).

[4] Han, S., Gomez-Flores, A., Choi, S., et al. "A study of nanofluid stability in low–salinity water to enhance oil recovery: An extended physicochemical approach" *Journal of Petroleum Science and Engineering* **215**(1), pp. 110608, (2022).

[5] Khashi'ie, NS., Waini, I., Kasim, AR., et al. "Thermal progress of a non-Newtonian hybrid nanofluid flow on a permeable Riga plate with temporal stability analysis" *Chinese Journal of Physics*, **77**(1), pp. 279-90, (2022).

[6] Sui, J., Zheng, L., Zhang, X., et al. "Mixed convection heat transfer in power law fluids over a moving conveyor along an inclined plate" *International Journal of Heat and Mass Transfer*, **85**(1), pp. 1023-33, (2015).

[7] Jalil, Mudassar, and Saleem Asghar. "Flow of power-law fluid over a stretching surface: A Lie group analysis" *International Journal of Non-Linear Mechanics*, **48**, pp. 65-71, (2013).

[8] Ahmed, J., Mahmood, T., Iqbal, Z., et al. "Axisymmetric flow and heat transfer over an unsteady stretching sheet in power law fluid" *Journal of Molecular Liquids*, **221**, pp. 386-93, (2016).

[9] Guha, Abhijit, and Kaustav Pradhan. "Natural convection of non-Newtonian power-law fluids on a horizontal plate" *International Journal of Heat and Mass Transfer*, **70**, pp. 930-938, (2014).

[10] Megahed, Ahmed M. "Flow and heat transfer of a non-Newtonian power-law fluid over a non-linearly stretching vertical surface with heat flux and thermal radiation" *Meccanica*, **50**(7), pp. 1693-1700, (2015).

[11] Saritha, K., M. Rajasekhar, and B. Reddy. "Heat and mass transfer of laminar boundary layer flow of non-Newtonian power law fluid past a porous flat plate with Soret and Dufour effects" *Physical science international journal*, **11**(1), pp. 1-13, (2016).

[12] Reddy, GJ., Raju, RS., Manideep, P., et al. "Thermal diffusion and diffusion thermo effects on unsteady MHD fluid flow past a moving vertical plate embedded in porous medium in the presence of Hall current and rotating system" *Transactions of A. Razmadze Mathematical Institute*, **170**(2), pp. 243-65, (2016).

[13] Mustafa, M., Hayat, T., Pop, I., et al. "Unsteady boundary layer flow of a Casson fluid due to an impulsively started moving flat plate" *Heat Transfer—Asian Research*, **40**(6), pp. 563-76, (2011).

[14] Bhattacharyya, Krishnendu, Tasawar Hayat, and Ahmed Alsaedi. "Analytic solution for magnetohydrodynamic boundary layer flow of Casson fluid over a stretching/shrinking sheet with wall mass transfer" *Chinese Physics B*, **22**(2), pp. 024702, (2013).

[15] Nadeem, Sohail, Rizwan Ul Haq, and C. Lee. "MHD flow of a Casson fluid over an exponentially shrinking sheet" *Scientia Iranica*, **19**(6), pp. 1550-1553, (2012).

[16] Fung, Yuan-Cheng, and Y. C. Fung. "Microcirculation" *Biodynamics: Circulation*, pp. 1550-1553, (1984).

[17] Mahdy, A., and Sameh E. Ahmed. "Unsteady natural convection heat and mass transfer of non-Newtonian Casson fluid along a vertical wavy surface" *International Journal of Mechanical and Mechatronics Engineering*, **11**(6), pp. 1284-1291, (2017).

[18] Opanuga AA, Adesanya SO, Okagbue HI, Agboola OO. "Impact of Hall current on the entropy generation of radiative MHD mixed convection casson fluid" *International Journal of Applied and Computational Mathematics*, **6**(1), pp. 1-8, (2020).

[19] Abbas, I., Hasnain, S., Alatawi, NA., et al. "Thermal radiation energy performance on stagnation-point flow in the presence of base fluids ethylene glycol and water over stretching sheet with slip boundary condition" *Energies*, **15**(21), pp. 7965, (2022).

[20] Chen, C-H. "Forced convection over a continuous sheet with suction or injection moving in a flowing fluid" *International Journal Acta Mechanica*, **1**38, pp. 1-11, (1999).

[21] Guedri, K., Ameer, Ahammad N., Nadeem, S., et al. "Insight into the heat transfer of third-grade micropolar fluid over an exponentially stretched surface" *Scientific Reports*, **12**(1), pp. 15577, (2022).

[22] Ejaz, A., Abbas, I., Nawaz, Y., et al. "Thermal Analysis of MHD Non-Newtonian Nanofluids over a Porous Media" *CMES-Computer Modeling in Engineering & Sciences*, **125**(3), pp. 1-13, (2020).

[23] Awan, AU., Majeed, S., Ali, B., et al. "Significance of nanoparticles aggregation and Coriolis force on the dynamics of Prandtl nanofluid: The case of rotating flow" *Chinese Journal of Physics*, **79**(1), pp. 264-74, (2022).

[24] AAwan, AU., Shah, NA., Ahmed, N., et al. "Analysis of free convection flow of viscous fluid with damped thermal and mass fluxes" *Chinese Journal of Physics*, **60**(1), pp. 98-106, (2019).

[25] Awan, Aziz Ullah, Syed Asif Ali Shah, and Bagh Ali. "Bio-convection effects on Williamson nanofluid flow with exponential heat source and motile microorganism over a stretching sheet" *Chinese Journal of Physics*, **1**, pp. 2795-2810, (2022).

[26] Awan, AU., Aziz, M., Ullah, N., et al. "Thermal analysis of oblique stagnation point flow with slippage on second-order fluid" *Journal of Thermal Analysis and Calorimetry*, pp. 1-3, (2021).

[27] Abbas, I., Hasnain, S., Alatawi, NA., et al. "Non-Newtonian nano-fluids in Blasius and Sakiadis flows influenced by magnetic field " *Nanomaterials*, **12**(23), pp. 4254, (2022).

[28] Awan, Aziz Ullah, Sana Abid, and Nadeem Abbas. "Theoretical study of unsteady oblique stagnation point based Jeffrey nanofluid flow over an oscillatory stretching sheet" *Advances in Mechanical Engineering*, **12**(11), pp. 971881, (2020).

[29] Awan, AU., Abid, S., Ullah, N., et al. "Magnetohydrodynamic oblique stagnation point flow of second grade fluid over an oscillatory stretching surface" *Results in Physics*, **18**(1), pp. 103233, (2020).

[30] Li, P., Z. Duraihem F., Awan, AU., et al. "Heat transfer of hybrid nanomaterials base Maxwell micropolar fluid flow over an exponentially stretching surface" *Nanomaterials*, **12**(7), pp. 1207, (2022).

[31] Akbar, AA., Awan, AU., Bani-Fwaz, MZ., et al. "Linear and quadratic convection significance on the dynamics of MHD Maxwell fluid subject to stretched surface" *Frontiers in Physics*, **1**, pp. 693, (2022).

[32] Shah, SA., Ahammad, NA., Ali, B., et al. "Significance of bio-convection, MHD, thermal radiation and activation energy across Prandtl nanofluid flow: A case of stretching cylinder" *International Communications in Heat and Mass Transfer*, **137**(1), pp. 106299, (2022).

[33] Khan, NS., Shah, Z., Islam, S., et al. "Entropy generation in MHD mixed convection non-Newtonian second-grade nanoliquid thin film flow through a porous medium with chemical reaction and stratification" *Entropy*, **21**(2), pp. 139, (2019).

[34] Shehzad, N., Zeeshan, A., Shakeel, M., et al. "Effects of magnetohydrodynamics flow on multilayer coatings of Newtonian and non-Newtonian fluids through porous inclined rotating channel" *Coatings*, **12**(4), pp. 430, (2022).

[35] Khashi'ie, NS., Waini, I., Arifin, NM., et al. "Dual solutions of unsteady two-dimensional electro-magneto-hydrodynamics (EMHD) axisymmetric stagnation-point flow of a hybrid nanofluid past a radially stretching/shrinking Riga surface with radiation effect" *International Journal of Numerical Methods for Heat & Fluid Flow*, **33**(1), pp. 333-50, (2023).

[36] Ramesh, GK., Prasannakumara, BC., Gireesha, BJ., et al. "Casson fluid flow near the stagnation point over a stretching sheet with variable thickness and radiation" *Journal of Applied Fluid Mechanics*, **9**(3), pp. 1115-022, (2016).

[37] Yahaya, RI., Md. Arifin N., Pop, I., et al. "Dual solutions for MHD hybrid nanofluid stagnation point flow due to a radially shrinking disk with convective boundary condition" *International Journal of Numerical Methods for Heat & Fluid Flow*, **33**(2), pp. 456-76, (2023).

[38] Sabir, Z., Imran, A., Umar, M., et al. "A numerical approach for 2-D Sutterby fluid-flow bounded at a stagnation point with an inclined magnetic field and thermal radiation impacts" *Thermal Science*, **25**(3 Part A), pp. 1975-87, (2021).

[39] Hussain, A., Rehman, A., Nadeem, S., et al. "A combined convection carreau–yasuda nanofluid model over a convective heated surface near a stagnation point: a numerical study" *Mathematical Problems in Engineering*, **1**, pp. 1-4, (2021).

[40] Oztop, HF., and Abu-Nada, E. "Numerical study of natural convection in partially heated rectangular enclosures filled with nanofluids" *International journal of heat and fluid flow*, **29**(5), pp. 1326-36, (2008).

[41] Hassanzadeh, R., and N. Tokgoz. "Thermal-hydraulic characteristics of nanofluid flow in corrugated ducts" *Journal of Engineering Thermophysics*, **26**(1), pp. 498-513, (2017).

[42] OKGÖZ, Nehir, Veli ÖZBOLAT, and Beşir ŞAHİN. "Investigation of Heat Transfer Enhancement by Using Al2O3/Water Nanofluid in Rectangular Corrugated Channel" *Kahramanmaras Sutcu Imam University Journal of Engineering Sciences*, **19**(2), pp. 42-51, (2016).

[43] Ozbolat, Veli, Nehir Tokgoz, and Besir Sahin. "Flow characteristics and heat transfer enhancement in 2D corrugated channels" *International Journal of Mechanical and Mechatronics Engineering*, **7**(10), pp. 2074-2078, (2013).

[44] Bilen, K., Tokgoz, N., Solmaz, I., et al. "Thermo-hydraulic performance of tube with decaying swirl flow generators" *Applied thermal engineering*, **200**, pp. 117643, (2022).

[45] Zheng, Liancun, Xinxin Zhang, and Jicheng He. "Suitable heat transfer model for self-similar laminar boundary layer in power law fluids" *Journal of Thermal Science*, **13**(1), pp. 150-154, (2004).

Biographies

Dr.Imran Abbas received the MSc. degree in mathematics from Preston University, Islamabad, Pakistan, in 2015, the M.S. degree in mathematics in Bahria University Islamabad, in 2019, and the Ph.D. degree from Air University Islamabad. His research interests include numerical analysis, Heat transfer, nanofluids, computational fluid dynamics, and finite difference schemes with emphasis on mathematical modeling and performance analysis

Dr.Shahid Hasnain obtained his degree from Linkoping University in Sweden in the year 2011. In 2017, he successfully defended his doctoral thesis at King Abdulaziz University in Saudi Arabia. He holds a Doctor of Sciences degree in Mathematics, which was awarded in 2017. The

individual's research interests encompass various areas of applied mathematics, with a specific focus on fluid mechanics and biology. In addition, he demonstrates expertise in partial differential equations, asymptotic methods, and inverse problems.

Dr.Muhammad Saqib received the B.S. degree in mathematics from International Islamic University, Islamabad, Pakistan, in 2008, the M.S. degree in mathematics in Sweden, in 2011, and the Ph.D. degree from King Abdulaziz University, Jeddah, Saudi Arabia, in 2017. He is currently an Assistant Professor in Khwaja Fareed University of Engineering & Information Technology, Rahim Yar Khan, Pakistan. His research interests include numerical analysis, nonlinear coupled systems, and finite difference schemes with emphasis on mathematical modeling and performance analysis.

Dr. Daoud S. Mashat is a Professor of Applied Mathematics at King Abdulaziz University (Jeddah). He graduated from Faculty of Science, King Abdulaziz University in Mathematic in 1405H and he was awarded a M.Sc. and a Ph.D. degree from Texas A & M University in 1991 and 1997, respectively. His research interests are in the Applied Mathematics, Numerical analysis and Elasticity.

figure caption

Fig.1 Geometrical setup of the problem

Fig.2 Variation in permeability have an impact on the velocity and temperature profiles.

Fig.3 several nanoparticles effects on the Nussle numbers for imperable

Fig.4 several nanoparticles effects on the Nussle numbers for injection

Fig.5 several nanoparticles effects on the Nussle numbers for suction

Fig.6 Impact of different nanoparticles on skin friction number for imperable

Fig.7 Impact of different nanoparticles on skin friction number for suction

Fig.8 Impact of different nanoparticles on skin friction number for injection

Fig.9 Effect of $f''(\eta)$ with φ for suction

Fig.10 Effect of $f''(\eta)$ with φ for injection

Fig.11 Effect of $f''(\eta)$ with φ for imperable

Fig.12 Effect of $f''(\eta)$ with f_w for imperable suction and injection

Fig.13 Effects of $f''(\eta)$ with magnetic field M

Fig.14 Effects of $f''(\eta)$ with ϵ imperable

Fig.15 Effects of $f''(\eta)$ with ϵ suction

Fig.16 Effects of $f''(\eta)$ with ϵ injectiont

Fig.17 Effects of $f''(\eta)$with β for suction

Fig.18 Effects of $f''(\eta)$with β for injection

Fig.19 Effects of $\theta''(\eta)$ with φ for imperable surface

Fig.20 Effects of $\theta''(\eta)$ with φ for suction

Fig.21 Effects of with n for suction

Fig.22 Effects of $f''(\eta)$ with n for injection

Table.1 Explore the variation $f''(\eta)$ at n = 0.85, for different values of the f_w.

Table.2 Numerical results of $f^{(''')}$, and for different values of β, M, ϵ, Pr, n